A new frequency domain system identification method

A A Stotsky
Signals and Systems, Chalmers University of Technology, Gothenburg SE-412 96, Sweden.
email: alexander.stotsky@chalmers.se

The manuscript was received on 9 January 2011 and was accepted after revision for publication on 17 March 2011.

DOI: 10.1177/0959651811406344

Abstract: A new frequency domain system identification method based on a multi-frequency input signal is proposed. Frequency contents of the oscillating signal are estimated using a modified Kaczmarz algorithm proposed in this paper. Lyapunov stability analysis is performed for this new Kaczmarz algorithm and transient bounds for estimation error are established. Moreover, a new method for estimation of the variance of the measurement noise in Kaczmarz algorithms is also described. A comparison of a transient performance of modified Kaczmarz algorithm and a recursive least-squares algorithm is presented. The results are applied to a frequency domain identification of a DC motor.

Keywords: frequency domain system identification, frequency response, Kaczmarz algorithm, strictly diagonally dominant matrix, persistence of excitation, DC motor, signal processing

1 INTRODUCTION

A property of a linear time-invariant system to be completely characterized by the steady-state response to harmonic input is the basis for the frequency domain system identification methods [**1**]. A harmonic input (a cosine wave) of a certain frequency applied to a linear system induces oscillations of the output of the same frequency with different magnitude and phase after some transient. The magnitude of the output signal is equal to the magnitude of the input signal multiplied by the module of the transfer function, and the phase shift is equal to the argument of the transfer function.

The frequency response of system can be measured by applying a test harmonic signal of a certain frequency and measuring magnitude and phase of the output signal at that frequency. This procedure is repeated for a number of frequencies in a specified frequency range and only one frequency at a time is used.

This method is time consuming since the response is measured *sequentially* (only one frequency at a time is used) for a number of frequencies. The identification method proposed in this paper applies a multi-frequency harmonic signal that contains a number of distinct frequencies, and the response is measured *simultaneously* at each frequency, recovering magnitude and phase. This in turn, essentially reduces a costly time of experiment, providing the same accuracy of estimation.

The model for the output signal is specified in a form of a trigonometric polynomial (a sum of sines and cosines of known frequencies specified in the input signal) with adjustable coefficients.

Many algorithms can be applied for estimation of the frequency contents of oscillating signals. One of such algorithms is a simple Kaczmarz algorithm [**2**] where the output of the model matches the measured signal exactly in each discrete step and the vector of the parameter mismatch is orthogonal to the regressor vector. The Kaczmarz algorithm was successfully tested for estimation of the frequency contents of the high-resolution engine speed signal [**3**] in automotive applications. A computational simplicity and robustness against a measurement noise make the Kaczmarz algorithm very attractive for estimation of the frequency contents of complex signals with a large number of frequencies in real-time applications. The Kaczmarz algorithm however, suffers from the following drawbacks: it neither allows the estimation of the variance of measurement noise nor selection of the order of a trigonometric polynomial in the case where new frequencies appear in the signal. A gain update algorithm with a forgetting factor is introduced in this paper aiming to the

performance improvement of a Kaczmarz projection method. Stability analysis is performed for the modified algorithm in this paper unlike in previous papers where similar modifications of the Kaczmarz algorithm were reported [**3**, **4**].

The performance of the modified Kaczmarz algorithm is compared in this paper to the performance of the recursive least-squares (RLS) algorithm. The modified algorithm is applied to the frequency domain identification of a DC motor.

The idea of using broadband excitation signals such as multi-sine signals for a frequency domain system identification was also discussed in [**5**] (see also references therein). The output of the system which is excited by a broadband signal is analysed via a standard fast Fourier transform (FFT) method that limits the frequencies of the input signal to the set of Fourier frequencies, i.e. a fundamental frequency accompanied by higher-frequency harmonics. Any distinct frequencies of the input signal can be used in the frequency domain system identification method described in this paper.

The contributions of this paper can be summarized as follows.

1. A new frequency domain system identification method based on a multi-frequency input signal applied to a frequency domain identification of DC motor.
2. A new Kaczmarz algorithm with a least-squares gain update for estimation of the frequency contents of the oscillating signals.
3. Lyapunov stability analysis for a new Kaczmarz algorithm with a least-squares gain update and transient bounds for estimation error.
4. A new method for estimation of the variance of the measurement noise in Kaczmarz algorithms.
5. A comparison of the performance of the modified Kaczmarz algorithm and a RLS algorithm.

This paper is organized as follows. A new frequency domain system identification method is proposed in the next section. A new modified Kaczmarz algorithm is introduced in section 3 and applied to a frequency domain identification of DC motor in section 4. The paper is concluded by a discussion presented in section 5.

2 A NEW FREQUENCY DOMAIN IDENTIFICATION METHOD BASED ON MULTI-FREQUENCY INPUT SIGNAL

A harmonic input u_k of a certain frequency q applied to a linear system with the frequency transfer function $H(\mathrm{i}q)$, where $\mathrm{i}^2 = -1$ induces oscillations of the output y_k of the same frequency q with different magnitude and phase after some transient. The magnitude of the output signal is equal to the magnitude of the input signal multiplied by the module of the transfer function, and the phase shift is equal to the argument of the transfer function.

The traditional method of the frequency response measurements is time consuming since the response is measured *sequentially* for a number of frequencies and only one frequency at a time is used. The identification method described in this section applies the composite harmonic signal to the input that contains the number of distinct frequencies, and the response is measured *simultaneously* at each frequency, recovering the magnitude and the phase.

The multi-frequency test input sequence u_k is chosen as

$$u_k = \sum_{q=q_1}^{q_n} A_q \cos(qk\Delta) \tag{1}$$

where A_q is the amplitude of harmonic signal at a frequency $q = q_1, \ldots, q_n$, n is the number of frequencies involved, $k = 0, 1, 2, \ldots$. An example of the multi-frequency test input sequence is shown in Fig. 6.

The principle of superposition implies that a sum of cosine waves as an input forces cosine waves at the output with the same frequencies after a transient and therefore discrete-time measurements of the output result in the sequence

$$y_k = \sum_{q=q_1}^{q_n} B_{q*} \cos(qk\Delta + \psi_{q*}) + \xi_k \tag{2}$$

where magnitude of the response is $B_{q*} = |H(\mathrm{i}q)|A_q$, and the phase $\psi_{q*} = \arg(H(\mathrm{i}q))$ are treated as uncertain parameters, where $|H(\mathrm{i}q)| = \frac{B_{q*}}{A_q}$ is the module/magnitude and $\arg(H(\mathrm{i}q))$ is the argument of the transfer function evaluated at a frequency q, and ξ_k is a zero mean white Gaussian measurement noise with a variance σ^2.

The output sequence (2) can be rewritten as

$$y_k = \sum_{q=q_1}^{q_n} a_{q*} \cos(qk\Delta) + b_{q*} \sin(qk\Delta) + \xi_k \tag{3}$$

where the relation between equations (2) and (3) is given by magnitude $B_{q*} = \sqrt{a_{q*}^2 + b_{q*}^2}$ and phase $\psi_{q*} = -\arctan\frac{b_{q*}}{a_{q*}}$, where a_{q*} and b_{q*} are unknown coefficients of the output trigonometric polynomial.

Finally, the output sequence can be presented in the vector form

$$y_k = \varphi_k^T \theta_* + \xi_k \tag{4}$$

where φ_k is the regressor and θ_* is the vector of constant unknown parameters defined as

$$\varphi_k^T = [\cos(q_1 k\Delta) \sin(q_1 k\Delta) \cos(q_2 k\Delta) \sin(q_2 k\Delta) \ldots \cos(q_n k\Delta) \sin(q_n k\Delta)] \tag{5}$$

$$\theta_*^T = [a_{q1*} b_{q1*} a_{q2*} b_{q2*} \ldots a_{qn*} b_{qn*}] \tag{6}$$

In other words the output sequence is presented in a form of trigonometric polynomial with known frequencies and unknown coefficients.

The model of the output sequence can be introduced as

$$\hat{y}_k = \varphi_k^T \theta_k \tag{7}$$

where φ_k is the regressor defined in (5) and θ_k is the following vector of adjustable parameters

$$\theta_k^T = [a_{q1k}\, b_{q1k}\, a_{q2k}\, b_{q2k} \ldots a_{qnk}\, b_{qnk}] \tag{8}$$

A *parameter estimation aim* is to find an update law for the parameter vector θ_k such that θ_k converges to θ_*, i.e. the following holds

$$E[\theta_k - \theta_*] = 0 \tag{9}$$

at steady state, provided that the regressor φ_k is persistently exciting, i.e. there exist positive constants ρ_0, ρ_1 and w such that the following inequality holds

$$0 < \rho_0 I \leqslant \sum_{p=k}^{p=k+w} \varphi_p \varphi_p^T \leqslant \rho_1 I \tag{10}$$

where E is a mathematical expectation and I is the identity matrix. Inequalities (10) are valid for any distinct frequencies of the input sequence provided that a zero division in the elements of the information matrix $\sum_{p=k}^{p=k+w} \varphi_p \varphi_p^T$ is avoided [**3**].

A frequency domain *system identification aim* is the convergence of the magnitude and phase

$$E[B_{qk} - B_{q*}] = 0 \tag{11}$$

$$E[\psi_{qk} - \psi_{q*}] = 0 \tag{12}$$

where

$$B_{qk} = \sqrt{a_{qk}^2 + b_{qk}^2} \tag{13}$$

$$\psi_{qk} = -\arctan\frac{b_{qk}}{a_{qk}} \tag{14}$$

and a_{qk} and b_{qk} are adjustable parameters defined in (8), $q = q_1, \ldots, q_n$ and $|\hat{H}(\mathrm{i}q)| = \left(\frac{B_{qk}}{A_q}\right)$.

The achievement of the system identification aim (11), (12) follows from the achievement of the parameter estimation aim (9) as can be shown using the linearization technique. Hence the system identification problem is reduced to the problem of estimation of the coefficients of a trigonometric polynomial.

Many algorithms can be applied to solve the parameter estimation problem (see for example the algorithms described in [**6**–**11**]), where the parameter convergence is granted by the condition of persistency of excitation (10). The faster the parameter convergence, the less time is required for a system identification, leading to the advantage of the proposed approach with respect to a conventional one. Therefore priority in this application should be given to the fast convergent algorithms leading to a rapid frequency domain system identification method.

3 A NEW MODIFIED KACZMARZ ALGORITHM

A new modified Kaczmarz algorithm is described in this section. First, the properties of the least-squares gain update algorithm are established in section 3.1. The modified Kaczmarz algorithm and transient bounds of estimation error are presented in section 3.2. A new method for estimation of a variance of measurement noise is described in section 3.3. Finally, a comparative analysis of the modified Kaczmarz algorithm and the RLS algorithm is performed in section 3.4.

3.1 A least-squares gain update with forgetting factor

Lemma 1
Consider the following gain update law

$$\Gamma_k^{-1} = \lambda_0 \Gamma_{k-1}^{-1} + \lambda_1 \varphi_k \varphi_k^T,\ \Gamma_0^{-1} = \gamma_0 I,\ \gamma_0 > 0, \tag{15}$$

where $k = 1, 2, 3, \ldots$ and $0 < \lambda_0 < 1$ is a *forgetting factor* and λ_1 is a gain factor with regressor vector φ_k. Then there exists a positive constant λ_{0*} sufficiently close to one such that for all λ_0 from the interval $\lambda_{0*} < \lambda_0 < 1$, and for a sufficiently large $\gamma_0 > 0$ the matrix Γ_k^{-1}, $k = 0, 1, 2, \ldots$ is a SDD matrix (a matrix is said to be a strictly diagonally dominant (SDD) matrix if in every row of the matrix, the magnitude

of the diagonal entry in that row is larger than the sum of the magnitudes of all the other (non-diagonal) entries in that row [**12**]), i.e. the following inequalities are valid

$$|\gamma_{ii}| > \sum_{j=1, j\neq i}^{2n+1} |\gamma_{ij}| \quad i = 1, \ldots, (2n+1) \tag{16}$$

for all admissible frequencies, where γ_{ij}, $i, j = 1, \ldots, (2n+1)$ are the elements of matrix Γ_k^{-1}, γ_{ii} are positive diagonal elements of matrix Γ_k^{-1} and n is the number of frequencies in signal (4).

Moreover, the matrix Γ_k^{-1} is a positive definite matrix, it has positive eigenvalues only for $k = 0, 1, 2, \ldots$ and the following inequalities are true

$$0 < \lambda_{\min}(\Gamma_k^{-1}) I \leqslant \Gamma_k^{-1} \leqslant \lambda_{\max}(\Gamma_k^{-1}) I \tag{17}$$

where $\lambda_{\min}(\Gamma_k^{-1}) > 0$ and $\lambda_{\max}(\Gamma_k^{-1}) > 0$ are minimal and maximal eigenvalues of the matrix Γ_k^{-1} respectively, and I is the identity matrix.

Finally, the following bounds are valid for minimal and maximal eigenvalues of the matrix Γ_k^{-1}

$$\lambda_{\min}(\Gamma_k^{-1}) \geqslant \min_i \{\gamma_{ii} - \sum_{j=1, j\neq i}^{2n+1} |\gamma_{ij}|\} > 0 \tag{18}$$

$$\lambda_{\max}(\Gamma_k^{-1}) \leqslant \max_i \{\gamma_{ii} + \sum_{j=1, j\neq i}^{2n+1} |\gamma_{ij}|\} \tag{19}$$

for $i = 1, \ldots, (2n+1)$.

Lemma 1 is proved via explicit evaluation of the elements of matrix Γ_k^{-1}. This evaluation is performed in Appendix 2.

Remark 1

Here and below extremely low frequencies q for which $\cos(q)$ is very close to one are not included in the set of admissible frequencies.

A Kaczmarz update law is modified in the next section with a least-squares gain update described above aiming to the performance improvement. The properties of matrix Γ_k^{-1} reported in Lemma 1 are very useful in stability analysis performed in section 3.2 where the matrix Γ_k^{-1} is used in a Lyapunov function candidate.

3.2 Kaczmarz projection algorithm with the gain update

Lemma 2

Consider the system (4), (7) with bounded measurement noise $|\xi_k| \leqslant c_\xi$, $c_\xi > 0$ and the following update law for θ_k

$$\theta_k = \theta_{k-1} + \frac{\Gamma_{k-1}\varphi_k}{\varphi_k^T \Gamma_{k-1} \varphi_k} (y_k - \theta_{k-1}^T \varphi_k) \tag{20}$$

$$\Gamma_k = \frac{1}{\lambda_0}\left[\Gamma_{k-1} - \frac{\Gamma_{k-1}\varphi_k\varphi_k^T\Gamma_{k-1}}{\left(\frac{\lambda_0}{\lambda_1} + \varphi_k^T\Gamma_{k-1}\varphi_k\right)}\right] \tag{21}$$

$$\Gamma_0 = \frac{1}{\gamma_0} I,\ \gamma_0 > 0,\ \frac{1}{2} < \lambda_0 < 1,\ \lambda_1 > 0$$

Then the following transient bound is valid for estimation error $\tilde{\theta}_k = \theta_k - \theta_*$

$$\| \tilde{\theta}_k \| \leqslant \sqrt{\frac{\lambda_0^k V_0 + b\frac{(1-\lambda_0^k)}{(1-\lambda_0)}}{\lambda_{\min}(\Gamma_k^{-1})}} \tag{22}$$

$$b = [\lambda_1 + \frac{\lambda_{ug}}{(n+1)} \frac{(1-\lambda_0)^2}{(2\lambda_0 - 1)} + \frac{\lambda_{ug}}{n+1}] c_\xi^2 \tag{23}$$

where $\lambda_{\min}(\Gamma_k^{-1})$ is a minimal eigenvalue of the matrix Γ_k^{-1} in step $k = 0, 1, 2, \ldots$ and λ_{ug} is a global upper bound for $\lambda_{\max}(\Gamma_k^{-1})$ that is $\lambda_{\max}(\Gamma_k^{-1}) \leqslant \lambda_{ug}$, $V_0 = \tilde{\theta}_0^T \Gamma_0^{-1} \tilde{\theta}_0$, $k = 0, 1, 2, \ldots$.

The proof of Lemma 2 is given in Appendix 3 and is based on the Lyapunov function $V_k = \tilde{\theta}_k^T \Gamma_k^{-1} \tilde{\theta}_k$, $k = 0, 1, 2, \ldots$ where Γ_k^{-1} is a positive definite and symmetric matrix with the properties described in Lemma 1.

Corollary

In the noise-free case, where $\xi_k = 0$ and $c_\xi = 0$ the following transient bound is valid

$$\| \tilde{\theta}_k \| \leqslant \sqrt{\frac{\lambda_0^k V_0}{\lambda_{\min}(\Gamma_k^{-1})}} \tag{24}$$

Remark 2

For the case where $\lambda_0 = 1$ the minimal eigenvalue of the matrix Γ_k^{-1} tends to infinity, that is $\lambda_{\min}(\Gamma_k^{-1}) \to \infty$ whereas $\lambda_{\min}(\Gamma_k^{-1})$ remain bounded for $\lambda_0 < 1$. Therefore $\| \tilde{\theta}_k \| \to 0$ as $k \to \infty$ in both cases due to (24).

Transient bound (22) cannot be made arbitrarily small when increasing $\lambda_{\min}(\Gamma_k^{-1})$ since λ_{ug} which is the upper bound for $\lambda_{\max}(\Gamma_k^{-1})$ ($\lambda_{\max}(\Gamma_k^{-1}) \leqslant \lambda_{ug}$, $k = 0, 1, 2, \ldots$) is also increasing in this case. The ratio $\frac{\lambda_{\max}(\Gamma_k^{-1})}{\lambda_{\min}(\Gamma_k^{-1})}$ is approximately constant at the steady-state for both $\lambda_0 = 1$ and $\lambda_0 < 1$.

The parameter mismatch $\tilde{\theta}_k$ and upper bound (22) are plotted in Fig. 1. This figure shows that the upper bound (22) obtained via the Lyapunov method is unfortunately very conservative.

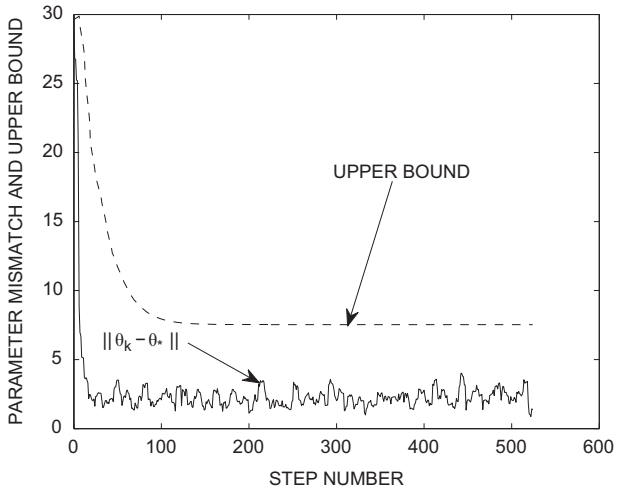

Fig. 1 Parameter mismatch $\| \tilde{\theta}_k \|$ and upper bound (22) are plotted as functions of a step number. The system (4), (20), (21) with the parameters $\lambda_0 = 0.95$, $\lambda_1 = 1$, $\gamma_0 = 10$, $q = 1, 2, 3$, $\sigma^2 = 3$, $c_\xi = 3\sigma$ was simulated

3.3 Estimation of a variance of measurement noise and an order of trigonometric polynomial

The method for estimation of the variance of the measurement noise σ^2 is based on relation (53) which relates the regressor vector, the vector of the parameter mismatch and measurement noise. The variance can be calculated due the fact that the algorithm is unbiased, i.e. a mathematical expectation of parameter vector is equal to a vector of true parameters at steady state [**13**].

Squaring both sides of (53) and taking mathematical expectation yields

$$E[\tilde{\theta}_k^T \varphi_k \varphi_k^T \tilde{\theta}_k] = E[\xi^2] = \sigma^2, \ \tilde{\theta}_k = \theta_k - \theta_* \tag{25}$$

The relation above gives the following estimate of the variance of the measurement noise

$$\hat{\sigma}^2 = \frac{1}{N} \sum_{k=1}^{N} (\theta_k - \bar{\theta})^T \varphi_k \varphi_k^T (\theta_k - \bar{\theta}) \tag{26}$$

where $\bar{\theta} = \frac{1}{N} \sum_{k=1}^{N} \theta_k$ is an average value of the parameter vector θ_k at steady state. The right-hand side of (26) is an estimate of the mathematical expectation $E[\tilde{\theta}_k^T \varphi_k \varphi_k^T \tilde{\theta}_k]$ where the vector of unknown parameters θ_* is replaced by the average value $\bar{\theta}$ ($E[\theta_k] = \theta_*$) for a sufficiently large sample size N at steady state.

This variance estimation technique (26) is based on estimation of a mathematical expectation which is well-estimated via a sample average for a sufficiently large sample size only. A histogram of an estimate of variance (26) plotted in Fig. 2 shows a pinpoint accuracy of estimation for a sufficiently large size.

Equation (26) is a useful tool for estimation of the order of trigonometric polynomial (4). The order of the polynomial should be increased (new frequencies should be added to a model) until estimate (26) of the variance of the measurement noise is reduced and this reduction is statistically significant.

3.4 Comparative analysis of the modified Kaczmarz algorithm and recursive least-squares algorithm

The modified Kaczmarz algorithm (20), (21) proposed in this paper is similar to RLS with a forgetting factor algorithm which can be written as follows [**1**]

$$\theta_k = \theta_{k-1} + \frac{\Gamma_{k-1} \varphi_k}{\lambda_0 + \varphi_k^T \Gamma_{k-1} \varphi_k} (y_k - \theta_{k-1}^T \varphi_k) \tag{27}$$

$$\Gamma_k = \frac{1}{\lambda_0} [\Gamma_{k-1} - \frac{\Gamma_{k-1} \varphi_k \varphi_k^T \Gamma_{k-1}}{(\lambda_0 + \varphi_k^T \Gamma_{k-1} \varphi_k)}] \tag{28}$$

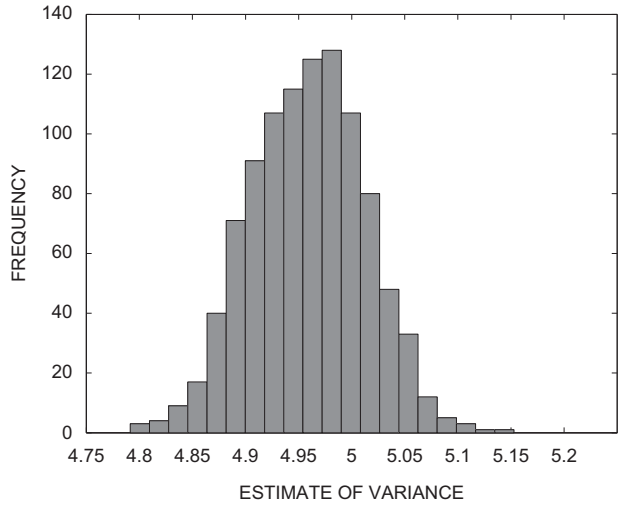

Fig. 2 Histogram plot which shows the frequencies of data points of an estimate of variance $\hat{\sigma}^2$ falling into discrete intervals (bins). The histogram estimates the probability density function of the variance $\hat{\sigma}^2$. The estimate of the variance $\hat{\sigma}^2$ is calculated using (26) with a sample size of $N = 17\,000$. The number of data points shown in histogram is equal to 1000, distributed over 20 bins. System (4), (20), (21) with a true variance $\sigma^2 = 5$ was simulated. An average value of the sample variance $\hat{\sigma}^2$ calculated using data shown in the histogram is equal to 4.9593 and a sample standard deviation is equal to 0.0539

where $0<\lambda_0 \leqslant 1$ is a forgetting factor. The matrix Γ_k is initialized to inverse of the information matrix after several initial steps and then updated recursively using (28).

The modified Kaczmarz algorithm (20), (21) and the RLS algorithm (27), (28) look very similar, but the matrix Γ_k plays a different role in these algorithms. This matrix is a gain matrix in the modified Kaczmarz algorithm (20), (21) whereas the matrix Γ_k is a recursive estimate of the inverse of the information matrix in the RLS algorithm (27), (28). The inverse of the information matrix can be calculated when this matrix gets a full rank. The modified Kaczmarz algorithm (20), (21) provides estimates which are close to correct values even at the initial steps whereas the RLS algorithm (27), (28) has a delay time until information matrix becomes invertible. The initial steps of two algorithms are shown in Fig. 3.

Notice that the matrix Γ_k in RLS algorithm can also be initialized in the same way as in algorithm (20), (21) and switched to the inverse of the information matrix after several initial steps. However, a stability analysis of the overall system is required in this case.

The robustness of the two algorithms against accumulation errors can be compared by adding an equal perturbation term $0.26I$, where I is a unity matrix, to the right-hand side of equations for the matrix Γ_k in (21) and (28). Estimates provided by the RLS algorithm oscillate whereas the modified Kaczmarz algorithm exhibits a robust behaviour and

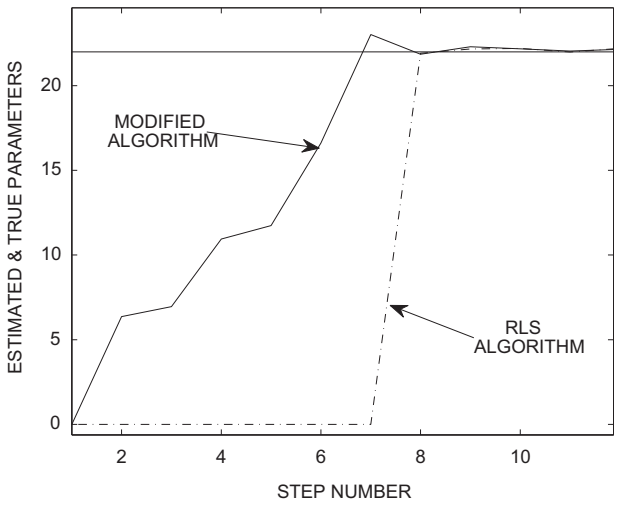

Fig. 3 System (4), (7) with $q = 1, 2, 3$, $\sigma^2 = 1$, was simulated with the modified Kaczmarz algorithm (20), (21) plotted with a solid line and the RLS algorithm (27), (28) plotted with a dash-dotted line. The two estimated parameters converge to the true value which is equal to 22

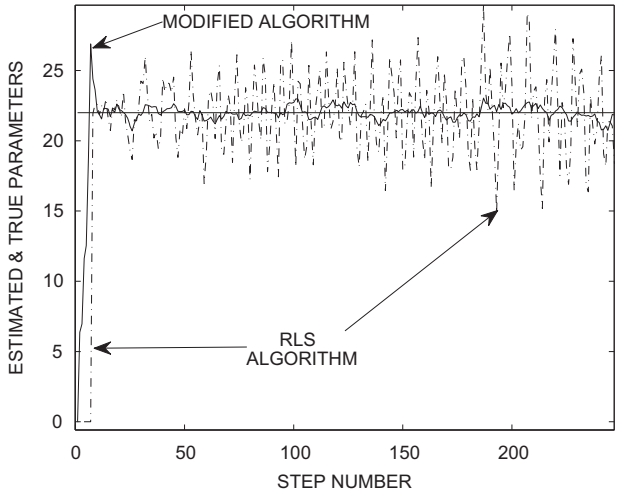

Fig. 4 System (4), (7) with $q = 1, 2, 3$, $\sigma^2 = 1$, was simulated with the modified Kaczmarz algorithm (20), (21) plotted with a solid line and the RLS algorithm (27), (28) plotted with a dash-dotted line. The two estimated parameters converge to the true value which is equal to 22

even a satisfactory performance as can be seen in Fig. 4. The error accumulation problem is well known for RLS algorithms and is discussed for example in reference [**14**]. As was mentioned earlier, the matrix Γ_k in the RLS algorithm is a recursive estimate of the inverse of the information matrix and errors in Γ_k destroy optimality and even might have an impact on the stability of the algorithm. In contrast, the matrix Γ_k in the modified Kaczmarz algorithm is treated just as a gain matrix which appears to be more tolerant of the error accumulation.

Finally, the three following algorithms: the Kaczmarz algorithm (20) with $\Gamma_k = I$, the modified Kaczmarz algorithm (20), (21), and the RLS algorithm (27), (28) are compared in terms of the variance of the parameter error $E \| \tilde{\theta}_k \|^2$. Figure 5 shows that the modified Kaczmarz algorithm and the Kaczmarz algorithm have the same variance of the parameter error for forgetting factors which are close to one. The modified Kaczmarz algorithm and the RLS algorithm show the same variance of the parameter error for forgetting factors which are smaller than 0.5. The RLS algorithm reduces the variance of the parameter error and shows better performance for forgetting factors which are close to one. However, the modified Kaczmarz algorithm is more robust with respect to accumulation errors and provides estimates which are close to the true values even at the initial steps of the algorithm. It can also be shown that the modified Kaczmarz algorithm converges much faster than the classical

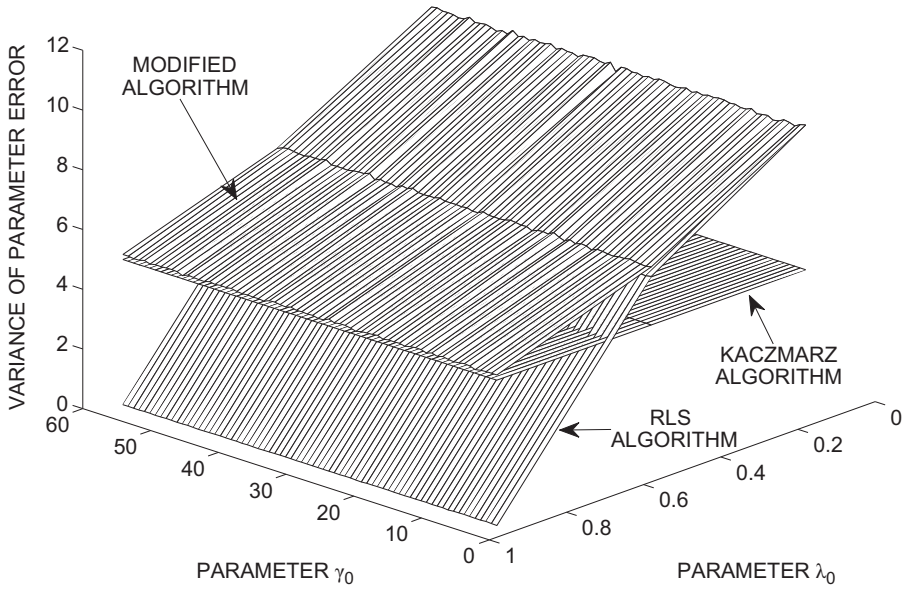

Fig. 5 A variance of the parameter mismatch $E \parallel \tilde{\theta}_k \parallel^2$ which is estimated at steady state via a sum of sample variances for a sufficiently large sample size. System (4), (7) with $q = 1, 2, 3$, $\sigma^2 = 3$ was simulated with the Kaczmarz algorithm (20) with $\Gamma_k = I$, the modified Kaczmarz algorithm (20), (21), and the RLS algorithm (27), (28). The variance is plotted as a function of the two parameters forgetting factor λ_0 and initial value γ_0 with $\lambda_1 = 1$

Kaczmarz algorithm. Therefore the modified algorithm is applied in the next section to frequency domain identification of a DC motor.

Note that the comparative analysis presented above is valid for a persistently exciting regressor vector for which inequalities (10) are valid. Kaczmarz algorithms might diverge in the absence of the persistence of excitation [**15**].

4 A FREQUENCY DOMAIN IDENTIFICATION METHOD OF DC MOTOR

DC motors are widely used as actuators in control systems to provide a rotary motion to a variety of electromechanical devices and servo systems. In order to achieve a high-performance regulation, the parameters of the motor should be identified. Newton's law combined with Kirchhoff's law yields the following transfer function of a DC motor, where the angle is the output and the voltage is the input

$$H(p) = \frac{K}{p(T_1 p + 1)(T_2 p + 1)} \tag{29}$$

where $T_1 = 0.1$ [s] and $T_2 = 0.02$ [s] are *mechanical* and *electrical* time constants respectively and $K = 100$ $\left[\frac{1}{s}\right]$ is a gain.

First, true values of the magnitude and the phase of the transfer function $H(iq)$ are calculated

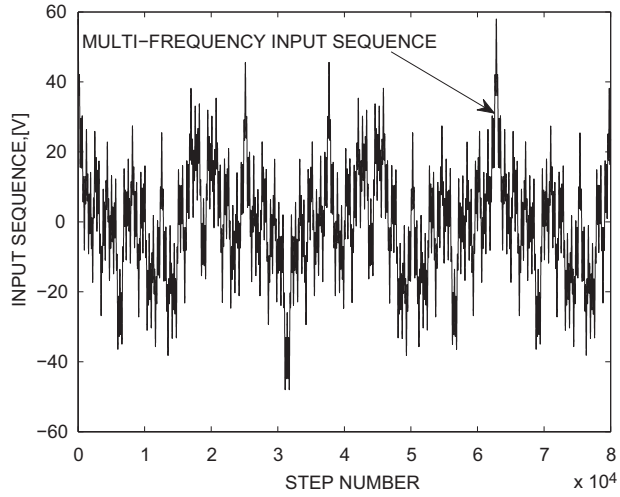

Fig. 6 The input multi-frequency test sequence u_k to DC motor is plotted as a function of a step number and specified in a form of trigonometric polynomial $u_k = \sum_{q=q_1}^{q=q_7} A_q \cos(qk\Delta)$, where $A_q = 10, 8, 8, 8, 8, 8, 8$ $[V]$ are the amplitudes at frequencies q=3,7,15,25,45,100,300$\left[\frac{1}{s}\right]$ respectively, Δ=0.0001, k=0,1,2,…

$$|H(iq)| = \frac{K}{q\sqrt{1 + q^2 T_1^2}\sqrt{1 + q^2 T_2^2}} \tag{30}$$

$$\psi_{q*} = -90^o - \arctan\frac{q(T_1 + T_2)}{1 - q^2 T_1 T_2} \tag{31}$$

Table 1 Frequency response

q, s^{-1}	0	3	7	15	25
$\lvert \mathrm{H(i}q) \rvert$	∞	31.87	11.59	3.54	1.33
$\lvert \hat{H}(\mathrm{i}q) \rvert$	∞	31.88	11.6	3.54	1.33
ψ_{q*},*Deg*	− 90	− 110.13	− 132.96	− 163.01	− 184.76
ψ_{qk},*Deg*	− 90	− 110.12	− 132.92	− 162.92	− 184.63
q, s^{-1}	45	100	150	∞	
$\lvert \mathrm{H(i}q) \rvert$	0.3583	0.0445	0.014	0	
$\lvert \hat{H}(\mathrm{i}q) \rvert$	0.3581	0.0449	0.0144	0	
ψ_{q*}, *Deg*	− 209.46	− 237.72	− 247.75	− 270	
ψ_{qk}, *Deg*	− 209.2	− 237.36	− 246.29	− 270	

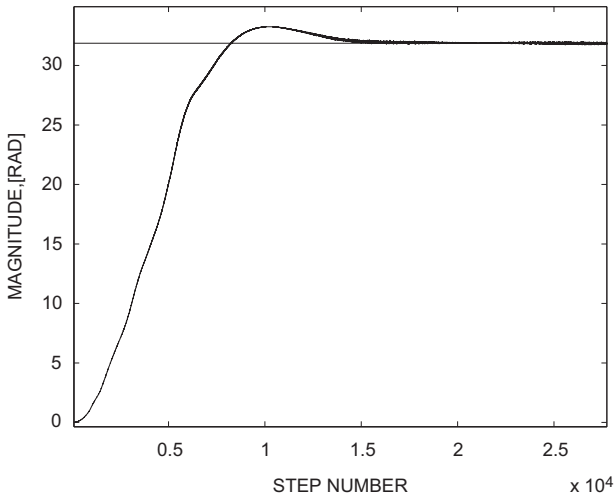

Fig. 7 The values of the magnitude $|\hat{H}(\mathrm{i}q)| = \frac{B_{qk}}{A_q}$ estimated via the modified algorithm (20), (21) are evaluated at frequency $q = 3\left[\frac{1}{\mathrm{s}}\right]$ and plotted as a function of a step number. A true value of the magnitude $|\mathrm{H(i}q)| = \frac{B_{q*}}{A_q}$ calculated via (30) is equal to 31.87

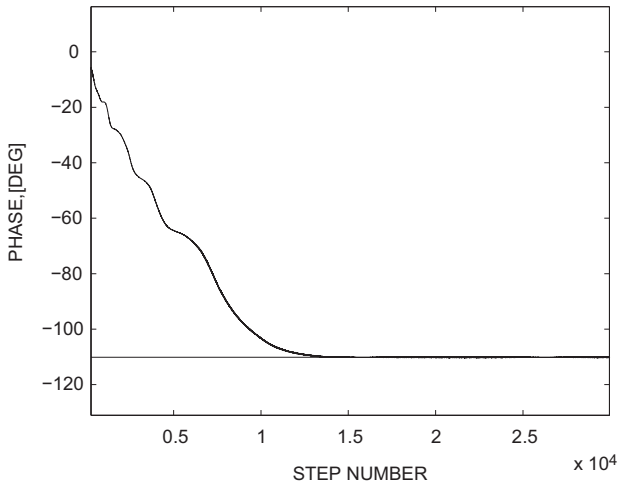

Fig. 8 The values of the phase $\psi_{qk} = -\arctan\frac{b_{qk}}{a_{qk}}$ estimated via modified algorithm (20), (21) are evaluated at frequency $q = 3\left[\frac{1}{\mathrm{s}}\right]$ and plotted as a function of a step number. A true value of the phase ψ_{q*} calculated via (31) is equal to -110.13°

for the following set of frequencies $q = 3, 7, 15, 25, 45, 100, 300\left[\frac{1}{\mathrm{s}}\right]$. Alternatively, the magnitude and the phase of the response can be calculated using a function *bode* of a Matlab software.

Second, the multi-frequency input sequence plotted in Fig. 6 is specified in a form of (1) and the model for the output is specified in a form of (7), where the parameters are updated via algorithm (20) and (21). A variance of the measurement noise is $\sigma^2 = 0.05$. Finally, the magnitude and the phase of the responses are calculated in Matlab using (13) and (14). The frequency responses for plant (29) are summarized in Table 1, where true values of the magnitude $|\mathrm{H(iq)}|$ and the phase ψ_{q*} calculated via (30), (31) are compared to the values of the magnitude $|\hat{H}(\mathrm{i}q)| = \left(\frac{B_{qk}}{A_q}\right)$ and the phase ψ_{qk} estimated via average value at steady state for 60 000 points using algorithm (20), (21). Table 1 shows very good agreement between estimated and true values of the magnitude and phase. Estimated values of the time constants and the gain for plant (29) can be calculated using the frequency response data listed in Table 1. Since the number of measured points is larger than the number of unknown parameters (two time constants and one gain) the estimated values of these parameters are over-determined and can be found using a least-squares method.

A transient performance of algorithm (20) and (21) is illustrated in Figs 7 and 8.

5 DISCUSSION

The methods that are able to rapidly solve the frequency response identification problems are very much in demand in such application areas as communication, instrumentation, civil engineering, biomedicine and others.

The performance of the transmission channels and cables is identified in communications by sending a test signal and recording the frequency response.

The frequency response curves of microphones, amplifiers, loudspeakers, CD players, and other devices can be identified in a similar way in the instrumentation area.

The frequency response functions of such civil engineering structures as buildings, towers, and bridges are used for active vibration mitigation and reduction of damaging effects of such dynamic loads as high winds, extreme waves, and strong earthquakes [**16**].

Frequency domain analysis can also be used in biomedical signal processing applications for rapid decomposition of rhythmic oscillations of the blood pressure and heart rate into different frequency components and for quantification of the power of these oscillations at each specific frequency [**17**].

Finally, radar/sonar and seismic signal processing applications should also be mentioned in a frequency domain context.

Simple, fast, and robust algorithms are required for estimation of the frequency components of multi-frequency output measurements in these and many other applications. The performance of the Kaczmarz algorithm is improved in this paper which makes the Kaczmarz projection method applicable to many problems as mentioned earlier.

FUNDING

This research received no specific grant from any funding agency in the public, commercial, or not-for-profit sectors.

REFERENCES

1 **Ljung, L.** *System identification: theory for the user*, 1999 (Prentice-Hall, Englewood Cliffs, New Jersey).
2 **Astrom, K. J.** and **Wittenmark, B.** *Adaptive control*, 1989 (Addison-Wesley, Reading, Massachusetts).
3 **Stotsky, A.** *Automotive engines: control, estimation, statistical detection*, 2009 (Springer, Berlin).
4 **Avedyan, E. D.** Modified Kaczmarz algorithms for estimating the parameters of linear plants. *Autom. Remote Control*, 1978, **39**(5), 674–680.
5 **Vandoorn, T., De Belie, F., Vyncke, T., Melkebeek, J.,** and **Lataire, P.** Generation of multi-sinusoidal test signals for the identification of synchronous-machine parameters by using a voltage-source inverter. *IEEE Trans. Industr. Electron.*, 2010, **57**(1), 430–439.
6 **Anderson, B. D. O., Bitmead, R. R., Jonson, C. R., Kokotovich, P. V., Kosut, R., Mareles, I. M. J., Praly, L.,** and **Riedle, B. D.** *Stability of adaptive systems: passivity and averaging analysis*, 1986 (MIT Press, Cambridge, Massachusetts).
7 **Goodwin, G.** and **Sin, K.** *Adaptive filtering, prediction and control*, 1984 (Prentice-Hall, Englewood Cliffs, New Jersey).
8 **Fomin, V. N., Fradkov, A. L.,** and **Yakubovich, V. A.** *Adaptive control of the dynamic plants*, 1981 (Nauka, Moscow) (in Russian).
9 **Iserman, R.** *Digital control systems*, 1981 (Springer, Berlin).
10 **Landau, I.** and **Zito, G.** *Digital control systems: design, identification and implementation*, 2006 (Springer, London).
11 **Sastry, S.** and **Bodson, M.** *Adaptive control: stability, convergence, and robustness*, Prentice-Hall Advanced Reference Series (Engineering), 1994 (Prentice-Hall, Englewood Cliffs, New Jersey).
12 **Horn, R.** and **Johnson, C.** *Matrix analysis*, 1985 (Cambridge University Press, Cambridge).
13 **Stotsky, A.** Recursive trigonometric interpolation algorithms. *Proc. IMechE, Part I: J. Systems and Control Engineering*, 2010, **224**(1), 65–77. DOI 10.1243/09596518JSCE823.
14 **Ljung, S.** and **Ljung, L.** Error propagation properties of recursive least-squares adaptation algorithms, *Automatica*, 1985, **21**(2), 157–167.
15 **Lefeber, E.** and **Polderman, J.** On the possible divergence of the projection algorithm. *IEEE Trans. Autom. Control*, 1995, **40**(3), 495–497.
16 **Jin, G., Sain, M.,** and **Spencer, B.** Frequency domain system identification for controlled civil engineering structures. *IEEE Trans. Control Syst. Technol.*, 2005, **13**(6), 1055–1062.
17 **Parati, G., Saul, J., Di Rienzo, M.,** and **Giuseppe Mancia, G.** Spectral analysis of blood pressure and heart rate variability in evaluating cardiovascular regulation. *Hypertension*, 1995, **25**, 1276–1286.

APPENDIX 1

Lemma 3

The following relationships are valid

$$\sum_{r=0}^{w}\lambda_0^{w-r}\cos(rq)=\frac{\lambda_0^{w+2}+\cos(wq)}{1+\lambda_0^2-2\lambda_0\cos(q)}+\frac{-\lambda_0^{w+1}\cos(q)-\lambda_0\cos((w+1)q)}{1+\lambda_0^2-2\lambda_0\cos(q)} \tag{32}$$

$$\sum_{r=0}^{w}\lambda_0^{w-r}\sin(rq)=\frac{\sin(wq)+\lambda_0^{w+1}\sin(q)}{1+\lambda_0^2-2\lambda_0\cos(q)}+\frac{-\lambda_0\sin((w+1)q)}{1+\lambda_0^2-2\lambda_0\cos(q)},\ 0<\lambda_0\leqslant 1 \tag{33}$$

$$\sum_{r=0}^{w}\lambda_0^{w-r}\cos^2(rq)=\frac{1}{2}\frac{(1-\lambda_0^{w+1})}{(1-\lambda_0)}+\frac{1}{2}\left[\frac{\lambda_0^{w+2}+\cos(2wq)-\lambda_0^{w+1}\cos(2q)}{1+\lambda_0^2-2\lambda_0\cos(2q)}+\frac{-\lambda_0\cos(2(w+1)q)}{1+\lambda_0^2-2\lambda_0\cos(2q)}\right] \tag{34}$$

$$\sum_{r=0}^{w}\lambda_0^{w-r}\sin^2(rq)=\frac{1}{2}\frac{(1-\lambda_0^{w+1})}{(1-\lambda_0)}-\frac{1}{2}\left[\frac{\lambda_0^{w+2}+\cos(2wq)-\lambda_0^{w+1}\cos(2q)}{1+\lambda_0^2-2\lambda_0\cos(2q)}+\frac{-\lambda_0\cos(2(w+1)q)}{1+\lambda_0^2-2\lambda_0\cos(2q)}\right] \tag{35}$$

$$\sum_{r=0}^{w}\lambda_0^{w-r}\cos^2(rq)+\sum_{r=0}^{w}\lambda_0^{w-r}\sin^2(rq)=\frac{(1-\lambda_0^{w+1})}{(1-\lambda_0)},\ 0<\lambda_0<1$$

Remark 3

Using relations presented above the following sums can easily be calculated

$$\sum_{r=0}^{w}\lambda_0^{w-r}\cos(rq_p)\cos(rq_l),$$

$$\sum_{r=0}^{w}\lambda_0^{w-r}\sin(rq_p)\sin(rq_l),$$

$$\sum_{r=0}^{w}\lambda_0^{w-r}\cos(rq_p)\sin(rq_l),\ p\neq l$$

Remark 4

The following sums $\sum_{r=0}^{w}\cos(rq)$, $\sum_{r=0}^{w}\sin(rq)$ reported in [**3**], [**13**] follow immediately from (32) and (33) with $\lambda_0=1$.

Proof

Consider the following sums

$$\sum_{r=0}^{w}\lambda_0^{w-r}e^{rq\mathrm{i}}=\lambda_0^{w}+\lambda_0^{w-1}e^{q\mathrm{i}}+\cdots+e^{wq\mathrm{i}} \tag{36}$$

$$\lambda_0 e^{-q\mathrm{i}}\left[\sum_{r=0}^{w}\lambda_0^{w-r}e^{rq\mathrm{i}}\right]=\lambda_0^{w+1}e^{-q\mathrm{i}}+\lambda_0^{w}+\cdots+\lambda_0 e^{(w-1)q\mathrm{i}} \tag{37}$$

where $\mathrm{i}^2=-1$. Subtraction of (37) from (36), where all the in-between terms vanish, yields

$$\sum_{r=0}^{w}\lambda_0^{w-r}e^{rq\mathrm{i}}=\frac{e^{wq\mathrm{i}}-\lambda_0^{w+1}e^{-q\mathrm{i}}}{1-\lambda_0 e^{-q\mathrm{i}}} \tag{38}$$

where $\lambda_0 e^{-q\mathrm{i}}\neq 1$.

Multiplication of the numerator and denominator of the ratio in the right-hand side of (38) by the following complex conjugate to denominator variable $(1-\lambda_0 e^{q\mathrm{i}})$ and subsequent decomposition of both sides of (38) into real and imaginary parts gives (32) and (33) when equating real and imaginary parts. Relations (34) and (35) follow directly from (32) and (33).

APPENDIX 2

Proof of Lemma 1

This lemma is proved via explicit evaluation of the elements of matrix Γ_k^{-1} defined in (15) using trigonometric relations reported in Lemma 3.

Equation

$$\Gamma_k^{-1}=\lambda_0\Gamma_{k-1}^{-1}+\lambda_1\varphi_k\varphi_k^T$$
$$\Gamma_0^{-1}=\gamma_0 I,\ \gamma_0>0,\ 0<\lambda_0<1,\lambda_1>0 \tag{39}$$

where I is the identity matrix, has the following solution

$$\Gamma_w^{-1}=\lambda_0^{w}\Gamma_0^{-1}+\lambda_1[\lambda_0^{w-1}\varphi_1\varphi_1^T+\lambda_0^{w-2}\varphi_2\varphi_2^T+\ldots+\varphi_w\varphi_w^T] \tag{40}$$

for $k=0,1,\ldots,w$, where

$$\varphi_k^T=[1\ \cos(q_1k\Delta)\ \sin(q_1k\Delta)\ \cos(q_2k\Delta)\ \sin(q_2k\Delta)\ldots\cos(q_nk\Delta)\ \sin(q_nk\Delta)] \tag{41}$$

where $\Delta=1$ for simplicity.

All the elements of the symmetric matrix Γ_k^{-1} at $k=w$ are evaluated

$$\Gamma_w^{-1}=\begin{bmatrix}\gamma_{11} & \gamma_{12} & \cdots\gamma_{1m}\\ \gamma_{21} & \gamma_{22} & \cdots\gamma_{2m}\\ \vdots & \vdots & \vdots\\ \gamma_{m1} & \gamma_{m2} & \cdots\gamma_{mm}\end{bmatrix}$$

where $m=2n+1$, n is the number of frequencies.

Evaluation of diagonal element γ_{11} yields

$$\gamma_{11}=\gamma_0\lambda_0^{w}+[\lambda_0^{w-1}+\lambda_0^{w-2}+\cdots+1]\lambda_1=(\gamma_0-\lambda_1)\lambda_0^{w}+\lambda_1\sum_{r=0}^{w}\lambda_0^{w-r}=(\gamma_0-\lambda_1)\lambda_0^{w}+\frac{\lambda_1(1-\lambda_0^{w+1})}{(1-\lambda_0)} \tag{42}$$

where $\gamma_0>\lambda_1+\frac{\lambda_1}{(1-\lambda_0)}$, and evaluation of element γ_{11} at steady-state yields

$$\gamma_{11}\to\frac{\lambda_1}{(1-\lambda_0)}\ as\ w\to\infty \tag{43}$$

provided that $0<\lambda_0<1$.

Notice that element γ_{11} can be made arbitrarily large if λ_0 is sufficiently close to one. Non-diagonal γ_{12} can be calculated as follows:

$$\gamma_{12} \to \lambda_1[\sum_{r=0}^{w} \lambda_0^{w-r} \cos(rq) - \lambda_0^w]$$
$$= {}^{(32)}\lambda_1[\frac{\lambda_0^{w+2} + \cos(wq) - \lambda_0^{w+1}\cos(q)}{1+\lambda_0^2 - 2\lambda_0\cos(q)} - \frac{\lambda_0\cos((w+1)q)}{1+\lambda_0^2-2\lambda_0\cos(q)} - \lambda_0^w] \quad (44)$$

where $q = q_1$ is the frequency.

Steady-state evaluation gives the relation

$$\gamma_{12} \to \lambda_1 \frac{\cos(wq) - \lambda_0\cos((w+1)q)}{1+\lambda_0^2-2\lambda_0\cos(q)} \quad as\ w \to \infty \quad (45)$$

provided that $0<\lambda_0<1$. Notice that element γ_{12} is bounded if λ_0 is sufficiently close to one.

The matrix Γ_w^{-1} is proved to be a SDD matrix as $w \to \infty$. Notice that a matrix is defined as a SDD matrix, if in every row of the matrix the magnitude of the diagonal entry in that row is larger than the sum of the magnitudes of all the other (non-diagonal) entries in that row. The diagonal dominance is verified row-wise. Consider the first row. The magnitude of the diagonal element in the first row γ_{11} should be larger than the sum of the magnitudes of all the other (non-diagonal) entries in that row. This means that element γ_{11} should be essentially larger in order to accommodate all non-diagonal elements) than the element $|\gamma_{12}|$ as $w \to \infty$. Two elements γ_{11} and $|\gamma_{12}|$ are plotted for $w = 150$ and $\lambda_1 = 1$ as functions of the frequency q and forgetting factor λ_0 and compared in Fig. 9. The elements are calculated using (43) and (45). Diagonal entry γ_{11} is larger than $|\gamma_{12}|$ for all admissible frequencies and forgetting factors and becomes essentially larger for all forgetting factors which are close to one. Notice that $\gamma_{11} = \gamma_{12}$ as $w \to \infty$ provided that $q = 0$ and the diagonal dominance is destroyed in this case.

Non-diagonal element γ_{13} can be evaluated as

$$\gamma_{13} = \lambda_1[\sum_{r=0}^{w} \lambda_0^{w-r}\sin(rq)] = \lambda_1 \frac{\sin(wq) + \lambda_0^{w+1}\sin(q) - \lambda_0\sin((w+1)q)}{1+\lambda_0^2-2\lambda_0\cos(q)} \quad (46)$$

Evaluation of element γ_{13} at steady-state gives the relation

$$\gamma_{13} \to \lambda_1[\frac{\sin(wq) - \lambda_0\sin((w+1)q)}{1+\lambda_0^2-2\lambda_0\cos(q)}] \quad as\ w \to \infty \quad (47)$$

provided that $0<\lambda_0<1$.

Using arguments similar to the arguments applied for evaluation of element γ_{12} it can be shown that diagonal element γ_{11} in the first row is significantly larger than the absolute value of γ_{13} if λ_0 is close to one. The next step is evaluation of remaining diagonal elements.

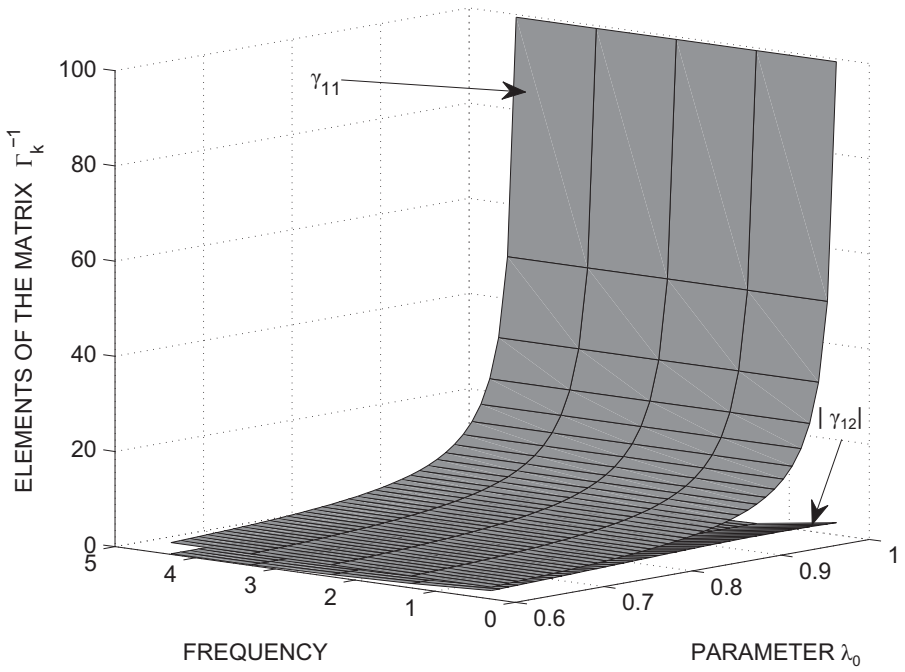

Fig. 9 Elements of the matrix Γ_k^{-1}. The diagonal entry γ_{11} and non-diagonal entry $|\gamma_{12}|$ are plotted for $k = w = 150$ and $\lambda_1 = 1$ as functions of the frequency q and forgetting factor λ_0. The diagonal entry γ_{11} is calculated using (43) and non-diagonal entry $|\gamma_{12}|$ is calculated using (45)

Evaluation of diagonal element γ_{22} yields

$$\gamma_{22} = \underbrace{(\gamma_0 - \lambda_1)\lambda_0^w + \frac{\lambda_1(1-\lambda_0^{w+1})}{2(1-\lambda_0)}}_{average\ part} + \underbrace{\frac{\lambda_1}{2}\left[\frac{\lambda_0^{w+2} + \cos(2wq) - \lambda_0^{w+1}\cos(2q)}{1+\lambda_0^2 - 2\lambda_0\cos(2q)}\right]}_{periodic\ part} - \underbrace{\frac{\lambda_0\cos(2(w+1)q)}{1+\lambda_0^2 - 2\lambda_0\cos(2q)}\Big]}_{periodic\ part} \quad (48)$$

and evaluation at steady-state gives the relation

$$\gamma_{22} \to \underbrace{\frac{\lambda_1}{2(1-\lambda_0)}}_{average\ part} + \underbrace{\frac{\lambda_1}{2}\left[\frac{\cos(2wq) - \lambda_0\cos(2(w+1)q)}{1+\lambda_0^2 - 2\lambda_0\cos(2q)}\right]}_{periodic\ part} \quad (49)$$

$as\ w \to \infty$

provided that $0<\lambda_0<1$.

Finally, diagonal element γ_{33} can be written as

$$\gamma_{33} = \underbrace{\underbrace{\gamma_0\lambda_0^w - \frac{\lambda_1\lambda_0^{w+1}}{2(1-\lambda_0)}}_{transient\ part} + \underbrace{\frac{\lambda_1}{2(1-\lambda_0)}}_{steady-state\ part}}_{average\ part} - \underbrace{\frac{\lambda_1}{2}\left[\frac{\lambda_0^{w+2} + \cos(2wq) - \lambda_0^{w+1}\cos(2q)}{1+\lambda_0^2 - 2\lambda_0\cos(2q)}\right]}_{periodic\ part} - \underbrace{\frac{\lambda_0\cos(2(w+1)q)}{1+\lambda_0^2 - 2\lambda_0\cos(2q)}\Big]}_{periodic\ part} \quad (50)$$

where

$$\gamma_0 > \frac{\lambda_1}{2(1-\lambda_0)}$$

and

$$\gamma_{33} \to \underbrace{\frac{\lambda_1}{2(1-\lambda_0)}}_{average\ part} - \underbrace{\frac{\lambda_1}{2}\left[\frac{\cos(2wq) - \lambda_0\cos(2(w+1)q)}{1+\lambda_0^2 - 2\lambda_0\cos(2q)}\right]}_{periodic\ part} \quad (51)$$

$as\ w \to \infty$

provided that $0<\lambda_0<1$. Relation (34) reported in Lemma 3 is used for calculation of elements (48) and (50).

Using similar arguments all other elements of the matrix Γ_w^{-1} can be calculated. Notice that the diagonal elements γ_{ii}, $i=2,3,\ldots,m$ defined in (48)–(51) have a periodic part and an average part, and all non-diagonal elements have a periodic part only. The average part in turn, consists of a transient part and a steady-state part where $w \to \infty$. Steady-state parts of all the diagonal elements γ_{ii}, $i=1,2,3,\ldots,m$ can be made sufficiently large as $\lambda_0 \to 1$, and all non-diagonal elements remain bounded as $\lambda_0 \to 1$ for all admissible frequencies q, i.e. for all frequencies excepting extremely low ones for which $\cos(q)$ is close to one. Therefore the matrix Γ_w^{-1} can be made an SDD matrix when $w \to \infty$ and $\lambda_0 \to 1$. Moreover, the matrix Γ_k^{-1} can also be made an SDD matrix at the transient for $k=0,1,2,\ldots,w$ for a sufficiently large $\gamma_0>0$ since γ_0 has impact on diagonal elements at transient only and all non-diagonal elements remain bounded. Therefore there exist λ_{0*} and a sufficiently large $\gamma_0>0$ such that for all $\lambda_{0*}<\lambda_0<1$ the matrix Γ_k^{-1} is an SDD matrix for all $k=0,1,2,\ldots$.

This symmetric SDD matrix Γ_k^{-1} with positive diagonal entries is positive definite, it has positive eigenvalues only and hence (17) holds due to the Rayleigh–Ritz theorem [**12**].

Gershgorin's circle theorem is a useful tool for estimation of the bounds for minimal and maximal eigenvalues of an SDD matrix Γ_k^{-1}. Around every diagonal element γ_{ii} of matrix Γ_k^{-1}, a circle with radius that is equal to the sum of the absolute values of the other elements on the same row is drawn. Such circles are called Gershgorin discs. Every eigenvalue λ of the matrix Γ_k^{-1} is located within at least one of the Gershgorin discs $D(\gamma_{ii}, R_i)$

$$|\lambda - \gamma_{ii}| \leqslant \sum_{j=1, j\neq i}^{2n+1} |\gamma_{ij}| \quad i=1,\ldots,(2n+1) \quad (52)$$

where γ_{ii} is the centre of the disc, and $R_i = \sum_{j=1, j\neq i}^{2n+1} |\gamma_{ij}|$ is the radius of the disc, n is the number of frequencies. The bounds for minimal and maximal eigenvalues of matrix Γ_k^{-1} (18) and (19) are defined as the end points of the Gershgorin discs.

Simulation results show that inequalities (18) and (19) provide sufficiently tight bounds for minimal and maximal eigenvalues of matrix Γ_k^{-1} respectively.

APPENDIX 3

Proof of Lemma 2

First notice that following relations are valid for system (4), (7) and (20), (21)

$$\varphi_k^T\tilde{\theta}_k=\xi_k \tag{53}$$

$$\tilde{\theta}_k-\tilde{\theta}_{k-1}=-\frac{\Gamma_{k-1}\varphi_k\varphi_k^T\tilde{\theta}_{k-1}}{\varphi_k^T\Gamma_{k-1}\varphi_k}+\frac{\Gamma_{k-1}\varphi_k}{\varphi_k^T\Gamma_{k-1}\varphi_k}\xi_k \tag{54}$$

$$\Gamma_k^{-1}=\lambda_0\Gamma_{k-1}^{-1}+\lambda_1\varphi_k\varphi_k^T \tag{55}$$

where $\tilde{\theta}_k=\theta_k-\theta_*$ is the parameter mismatch and θ_* is the vector of true parameters.

Consider the following Lyapunov function candidate

$$V_k=\tilde{\theta}_k^T\Gamma_k^{-1}\tilde{\theta}_k \tag{56}$$

which is equal to

$$V_k=\tilde{\theta}_k^T\Gamma_{k-1}^{-1}\tilde{\theta}_k^T-(1-\lambda_0)\tilde{\theta}_k^T\Gamma_{k-1}^{-1}\tilde{\theta}_k^T+\lambda_1\xi_k^2 \tag{57}$$

due to (53) and (55), where Γ_k^{-1} is a positive definite and symmetric matrix whose properties are described in Lemma 1.

Evaluation of the first difference yields

$$\begin{aligned}V_k-V_{k-1}&=\tilde{\theta}_k^T\Gamma_{k-1}^{-1}\tilde{\theta}_k^T-\tilde{\theta}_{k-1}^T\Gamma_{k-1}^{-1}\tilde{\theta}_{k-1}^T\\&\quad-(1-\lambda_0)\tilde{\theta}_k^T\Gamma_{k-1}^{-1}\tilde{\theta}_k^T+\lambda_1\xi_k^2\\&=(\tilde{\theta}_k+\tilde{\theta}_{k-1})^T\Gamma_{k-1}^{-1}(\tilde{\theta}_k-\tilde{\theta}_{k-1})\\&\quad-(1-\lambda_0)\tilde{\theta}_k^T\Gamma_{k-1}^{-1}\tilde{\theta}_k^T+\lambda_1\xi_k^2\\&=-(\tilde{\theta}_k+\tilde{\theta}_{k-1})^T\Gamma_{k-1}^{-1}[\frac{\Gamma_{k-1}\varphi_k\varphi_k^T\tilde{\theta}_{k-1}}{\varphi_k^T\Gamma_{k-1}\varphi_k}\\&\quad-\frac{\Gamma_{k-1}\varphi_k}{\varphi_k^T\Gamma_{k-1}\varphi_k}\xi_k]-(1-\lambda_0)\tilde{\theta}_k^T\Gamma_{k-1}^{-1}\tilde{\theta}_k^T+\lambda_1\xi_k^2\\&=-\tilde{\theta}_k^T\frac{\varphi_k\varphi_k^T}{\varphi_k^T\Gamma_{k-1}\varphi_k}\tilde{\theta}_{k-1}-\tilde{\theta}_{k-1}^T\frac{\varphi_k\varphi_k^T}{\varphi_k^T\Gamma_{k-1}\varphi_k}\tilde{\theta}_{k-1}\\&\quad+\tilde{\theta}_k^T\frac{\varphi_k\xi_k}{\varphi_k^T\Gamma_{k-1}\varphi_k}+\tilde{\theta}_{k-1}^T\frac{\varphi_k\xi_k}{\varphi_k^T\Gamma_{k-1}\varphi_k}\\&\quad-(1-\lambda_0)\tilde{\theta}_k^T\Gamma_{k-1}^{-1}\tilde{\theta}_k^T+\lambda_1\xi_k^2\end{aligned}$$

Taking into account (53) the difference V_k-V_{k-1} is written as

$$\begin{aligned}V_k-V_{k-1}=&-\tilde{\theta}_{k-1}^T\frac{\varphi_k\varphi_k^T}{\varphi_k^T\Gamma_{k-1}\varphi_k}\tilde{\theta}_{k-1}\\&-(1-\lambda_0)\tilde{\theta}_k^T\Gamma_{k-1}^{-1}\tilde{\theta}_k^T+\left[\lambda_1+\frac{1}{\varphi_k^T\Gamma_{k-1}\varphi_k}\right]\xi_k^2\end{aligned} \tag{58}$$

Notice that transient bound (67) where $\lambda_0=1$ follows immediately from (58) with $\xi_k=0$.

Evaluation of the term $-(1-\lambda_0)\tilde{\theta}_k^T\Gamma_{k-1}^{-1}\tilde{\theta}_k^T$ using (53) and (54) yields

$$\begin{aligned}&-(1-\lambda_0)\tilde{\theta}_k^T\Gamma_{k-1}^{-1}\tilde{\theta}_k^T=-(1-\lambda_0)\\&\left[\tilde{\theta}_{k-1}-\frac{\Gamma_{k-1}\varphi_k\varphi_k^T\tilde{\theta}_{k-1}}{\varphi_k^T\Gamma_{k-1}\varphi_k}+\frac{\Gamma_{k-1}\varphi_k}{\varphi_k^T\Gamma_{k-1}\varphi_k}\xi_k\right]^T\\&\Gamma_{k-1}^{-1}\left[\tilde{\theta}_{k-1}-\frac{\Gamma_{k-1}\varphi_k\varphi_k^T\tilde{\theta}_{k-1}}{\varphi_k^T\Gamma_{k-1}\varphi_k}+\frac{\Gamma_{k-1}\varphi_k}{\varphi_k^T\Gamma_{k-1}\varphi_k}\xi_k\right]=\\&-(1-\lambda_0)[\tilde{\theta}_{k-1}^T\Gamma_{k-1}^{-1}\tilde{\theta}_{k-1}-2\tilde{\theta}_{k-1}^T\frac{\varphi_k\varphi_k^T}{\varphi_k^T\Gamma_{k-1}\varphi_k}\tilde{\theta}_{k-1}\\&+2\tilde{\theta}_{k-1}^T\frac{\varphi_k\xi_k}{\varphi_k^T\Gamma_{k-1}\varphi_k}+\tilde{\theta}_{k-1}^T\varphi_k\varphi_k^T\tilde{\theta}_{k-1}\\&-2\tilde{\theta}_{k-1}^T\varphi_k\xi_k+\xi_k^2]\end{aligned} \tag{59}$$

Relation (59) contains two cross-terms

$$-2(1-\lambda_0)\tilde{\theta}_{k-1}^T\frac{\varphi_k\xi_k}{\varphi_k^T\Gamma_{k-1}\varphi_k}$$

and

$$2(1-\lambda_0)\tilde{\theta}_{k-1}^T\varphi_k\xi_k$$

which depend on noise ξ_k and should be overbounded. Taking into account the following inequalities

$$\begin{aligned}&-2(1-\lambda_0)\tilde{\theta}_{k-1}^T\frac{\varphi_k\xi_k}{\varphi_k^T\Gamma_{k-1}\varphi_k}\\&\leqslant(2\lambda_0-1)\tilde{\theta}_{k-1}^T\frac{\varphi_k\varphi_k^T}{\varphi_k^T\Gamma_{k-1}\varphi_k}\tilde{\theta}_{k-1}\\&+\frac{(1-\lambda_0)^2}{2\lambda_0-1}\frac{\xi_k^2}{\varphi_k^T\Gamma_{k-1}\varphi_k},\\&2(1-\lambda_0)\tilde{\theta}_{k-1}^T\varphi_k\xi_k\leqslant(1-\lambda_0)\tilde{\theta}_{k-1}^T\varphi_k\varphi_k^T\tilde{\theta}_{k-1}\\&+(1-\lambda_0)\xi_k^2\end{aligned}$$

where $\frac{1}{2}<\lambda_0<1$, and the following identities

$$[-1+2(1-\lambda_0)+(2\lambda_0-1)]\tilde{\theta}_{k-1}^T\frac{\varphi_k\varphi_k^T}{\varphi_k^T\Gamma_{k-1}\varphi_k}\tilde{\theta}_{k-1}=0$$

$$[(1-\lambda_0)-(1-\lambda_0)]\tilde{\theta}_{k-1}^T\varphi_k\varphi_k^T\tilde{\theta}_{k-1}=0$$

evaluation of the first difference $V_k - V_{k-1}$ (58) yields

$$V_k - V_{k-1} \leqslant -(1-\lambda_0)\tilde{\theta}_{k-1}^T\Gamma_{k-1}^{-1}\tilde{\theta}_{k-1}^T + [\lambda_1 + \frac{(1-\lambda_0)^2}{(2\lambda_0-1)\varphi_k^T\Gamma_{k-1}\varphi_k} + \frac{1}{\varphi_k^T\Gamma_{k-1}\varphi_k}]\xi_k^2 \quad (60)$$

and

$$V_k \leqslant \lambda_0 V_{k-1} + b \quad (61)$$

$$b = [\lambda_1 + \frac{\lambda_{ug}}{(n+1)}\frac{(1-\lambda_0)^2}{(2\lambda_0-1)} + \frac{\lambda_{ug}}{n+1}]c_\xi^2 \quad (62)$$

where $|\xi_k| \leqslant c_\xi$, c_ξ is a positive constant,

$$\varphi_k^T\Gamma_{k-1}\varphi_k \geqslant \frac{\varphi_k^T\varphi_k}{\lambda_{\max}(\Gamma_{k-1}^{-1})} = \frac{n+1}{\lambda_{\max}(\Gamma_{k-1}^{-1})} \geqslant \frac{n+1}{\lambda_{ug}} > 0,$$

where $\lambda_{\max}(\Gamma_{k-1}^{-1}) \leqslant \lambda_{ug}$, where $\lambda_{\max}(\Gamma_{k-1}^{-1})$ and $\lambda_{ug} > 0$ are maximal eigenvalue of Γ_{k-1}^{-1} and its global upper bound respectively, $k = 1, 2, \ldots$ and minimal eigenvalue of the matrix Γ_{k-1} is the same as the inverse (reciprocal) of the maximal eigenvalue of the matrix Γ_{k-1}^{-1}.

A solution of inequality (61) gives the following bound

$$V_k \leqslant \lambda_0^k V_0 + b[1 + \lambda_0 + \lambda_0^2 + \cdots + \lambda_0^{k-1}] \quad (63)$$

where $V_0 = (\theta_0 - \theta_*)^T\Gamma_0^{-1}(\theta_0 - \theta_*)$ and a positive constant b is given in (62). Calculation of the sum of geometric progression yields

$$V_k \leqslant \lambda_0^k V_0 + b\frac{(1-\lambda_0^k)}{(1-\lambda_0)} \quad (64)$$

Finally, taking into account (17) the transient bound for the parameter mismatch $\tilde{\theta}_k$ can be written as

$$\| \tilde{\theta}_k \| \leqslant \sqrt{\frac{\lambda_0^k V_0 + b\frac{(1-\lambda_0^k)}{(1-\lambda_0)}}{\lambda_{\min}(\Gamma_k^{-1})}}, \quad (65)$$

$$b = [\lambda_1 + \frac{\lambda_{ug}}{(n+1)}\frac{(1-\lambda_0)^2}{(2\lambda_0-1)} + \frac{\lambda_{ug}}{n+1}]c_\xi^2 \quad (66)$$

where $\lambda_{\min}(\Gamma_k^{-1})$ is a minimal eigenvalue of the matrix Γ_k^{-1} in step $k = 0, 1, 2, \ldots$.

In the noise-free case, where $\xi_k = 0$ and $c_\xi = 0$ the following transient bound is valid

$$\| \tilde{\theta}_k \| \leqslant \sqrt{\frac{\lambda_0^k V_0}{\lambda_{\min}(\Gamma_k^{-1})}} \quad (67)$$